Biochimica et Biophysica Acta 1787 (2009) 697–705

Contents lists available at ScienceDirect

Biochimica et Biophysica Acta

journal homepage: www.elsevier.com/locate/bbabio

Solid-state NMR and functional studies on proteorhodopsin

Nicole Pfleger, Andreas C. Wörner, Jun Yang, Sarika Shastri, Ute A. Hellmich, Lubica Aslimovska, Melanie S.M. Maier, Clemens Glaubitz *

Centre for Biomolecular Magnetic Resonance, Cluster of Excellence Macromolecular Complexes, Institute for Biophysical Chemistry, Goethe University Frankfurt, Max von Laue Str. 9, 60438 Frankfurt/M., Germany

ARTICLE INFO

Article history:
Received 14 January 2009
Received in revised form 16 February 2009
Accepted 17 February 2009
Available online 5 March 2009

Keywords:
Proteorhodopsin
Solid-state NMR
AFM
Cryo EM
Reconstitution
Proton transport
Histidine
HETCOR
Bound water

ABSTRACT

Proteins of the proteorhodopsin (PR) family are found abundantly in many marine bacteria in the photic zone of the oceans. They are colour-tuned to their environment. The green absorbing species has been shown to act as a light-driven proton pump and thus could form a potential source of energy. The pK_a of the primary proton acceptor is close to the pH of seawater which could also indicate a regulatory role. Here, we review and summarize our own recent findings in the context of known data and present some new results. Proton transfer *in vitro* by PR is shown by a fluorescence assay which confirms a pH dependent vectoriality. Previously reported low diffracting 2D crystal preparations of PR are assessed for their use for solid-state NMR by two dimensional ^{13}C–^{13}C DARR spectra. ^{15}N–^{1}H HETCOR MAS NMR experiments show bound water in the vicinity of the protonated Schiff base which could play a role in proton transfer. The effect of highly conserved H75 onto the properties of the chromophore has been investigated by single site mutations. They do show a pronounced effect onto the optical absorption maximum and the pK_a of the proton acceptor but have only a small effect onto the ^{15}N chemical shifts of the protonated Schiff base.

1. Introduction

Proteorhodopsin (PR) is a retinylidene membrane protein found in the genomes of many species of marine proteobacteria in the photic zone of the oceans [1,2]. Many hundred variants have been found which share 80% sequence identity but show different absorption maxima shifted by up to 35 nm between green and blue [3]. Especially the green absorbing form (27 kDa, λ_{max} ~520 nm) has been in the focus of a number of studies.

Green proteorhodopsin (PR) shares a 30% sequence identity with bacteriorhodopsin (BR). The primary proton acceptor D85, the proton donor D96, the Schiff base linkage K216 and the counterions of the Schiff base R82 and D212 in BR correspond to D97, E108, K231, R94 and D227 in PR, respectively as shown in Fig. 1 [4,5]. In contrast to BR, PR has no ionisable extracellular groups for a fast release of protons to the extracellular media. The residue H75 is highly conserved within the PR family and predicted to be close to the photoactive site potentially playing an important role in proton transfer, but it is missing in BR [5]. Topology analysis and homology modelling predicts the typical architecture of 7 transmembrane helices for residues 25 to 249.

It is well established that green PR works as a light-driven proton pump *in vitro* and *in vivo* when expressed in ooyctes [4] or *Escherichia coli* cells [6]. This observation together with the widespread occurrence of PR in marine bacteria suggests an important energetic role in addition to chlorophyll-based photosynthesis in the oceans. However, these observations might not reflect the true gene function *in situ* and clear evidence for the benefit of PR for marine bacteria under oligotrophic conditions is still lacking [7]. It is also interesting to note, that the pK_a of the primary proton acceptor in PR is close to the pH of sea water and five pH units higher than that found in BR (PR: p$K_{a,D97}$ ~7.5, bR: p$K_{a,\ D85}$ ~2.5) [4], which could be an indicator for a regulatory function. The sequence diversity within the PR family is comparable to the differences between archaeal proton-pumping and sensory rhodopsins, so it might be possible that these proteins fulfill an array of physiological functions [7].

PR undergoes a photocycle with a short turnover time of about 20 ms which contains K, M, N and O intermediates [8]. The photocycle has been studied spectroscopically at different time scales in some detail [3,8–15] but except for low-resolution AFM and EM data [16,17] no structural data are available yet. However, solid-state NMR has

Abbreviations: AFM, atomic force microscopy; BLM, black lipid membranes; BR, Bacteriorhodopsin; CP, cross polarisation; CS, chemical shift; DARR, dipolar assisted rotational resonance; DCP, double cross polarisation; DMPC, 1,2-dimyristoyl-sn-glycero-3-phosphocholine; EM, electron microscopy; FTIR (spectroscopy), Fourier Transform Infrared (spectroscopy); HETCOR, heteronuclear correlation; HPTS, 8-Hydroxypyrene-1,3,6-trisulfonic acid; MAS, magic angle spinning; NMR, nuclear magnetic resonance; POPC, 1-palmitoyl-2-oleoyl-sn-glycero-3-phosphocholine; POPG, 1-palmitoyl-2-oleoyl-sn-glycero-3-phosphoglycerol; PR, Proteorhodopsin; (p)SB, (protonated) Schiff base

* Corresponding author. Tel.: +49 69 798 29927; fax: +49 69 798 29929.
E-mail address: glaubitz@em.uni-frankfurt.de (C. Glaubitz).

0005-2728/$ – see front matter © 2009 Elsevier B.V. All rights reserved.
doi:10.1016/j.bbabio.2009.02.022

Fig. 1. Alignment of PR and BR using CLUSTALW reveals 23% identity, 20% strongly similar and 10% weakly similar residues in both sequences. Interestingly, H75 is highly conserved within the PR family but not found in bR (b), while a primary proton acceptor (c), a proton donor (d) and the Schiff base linkage (e) are found in both cases (PR: D97, E108, K231; BR: D85, D96, K216). The first 18 residues in PR are predicted as signal peptide in which V10 and I11 (a) form a unique pair which was used to identify this extended N-terminus *in vitro* (see text).

been used to probe the photoactive centre of PR. It has been shown, that the retinal exists in the ground state mainly in its all-*trans* configuration. The pH dependent protonation state of the Schiff base has been determined in comparison to D97N showing a very high pK_a for the pSB [18]. Furthermore residue selectively labelled samples have been used to probe sidechain and backbone dynamics in 2D crystalline PR samples [17].

In the following, we present new data on three different aspects of PR: in the first part, the issue of opposite proton transfer direction under acidic and alkaline conditions is addressed using a fluorescence based *in vitro* assay. In the second part, we compare previously obtained EM and AFM data, present 2D solid-state NMR spectra and discuss possible sources of sample inhomogeneities. The third part is dedicated to solid-state NMR data on the effect of H75 onto the Schiff base chemical shift and protonation state. Furthermore, we show that bound water exists in close proximity to the pSB.

2. Results and discussions

2.1. A new in vitro experiment to show pH dependent proton transfer by PR

Proton pumping of PR has been investigated in some details in reconstituted as well as cellular systems. Due to the considerable homologies of amino acids responsible for vectorial proton transfer and those forming the retinal binding pocket between BR and PR, a similar mechanism for light-driven proton transfer has been assumed. However, this comparison only holds true at alkaline pH due to the very high pK_a of D97 in PR (~7.5). At acidic pH, it has been difficult to observe an M-like state with a de-protonated Schiff base [4,19] and the direction of proton pumping was found to be inverted as seen by photocurrent measurements in reconstituted liposomes attached to BLM and in oocytes under voltage clamp conditions [4]. These findings were challenged by experiments reported by others [19,20].

2.1.1. Results and discussion

Here, we confirm in a simple *in vitro* experiment, that green PR transfers protons and that the direction of proton transfer can indeed be reversed in a pH dependent manner. The basic idea of this experiment is shown in Fig. 2a: PR solubilised in DDM with a C-terminal His-tag binds to Ni–NTA coated silicate particles with 0.2 μm diameter. PR bound to these beads was reconstituted into detergent destabilised, preformed POPC/POPG (5:1) lipid vesicles in the presence of the pH sensitive fluorophore HPTS. The size of the silicate beads will enforce a net C_{out}–N_{in} (outside-in) orientation of PR. Detergent was removed by biobeads, the silicate beads were removed by adding imidazole and subsequent centrifugation. Free HPTS was removed by dialysis. This procedure results in a system with outside-in PR liposomes with HPTS inside (Fig. 2a). This dye is a well established pH sensitive fluorophore with a pK_a of 7.3 [21]. A pH increase causes an increase of its fluorescence quantum yield. When the sample is illuminated with green light at an alkaline pH above the main pK_a of PR, protons should be pumped inside causing an acidification of the lumen. This results in fluorescence decrease of HPTS, which can only be detected after the green light source is switched when the system returns to equilibrium due to proton leakage (Fig. 2b, right). The opposite should be expected at acidic pH if the direction of proton transfer is reversed (Fig. 2b, left). Experimental data for wt PR are shown in Fig. 2c. HPTS fluorescence was excited at 460 nm and detected at 514 nm. PR was illuminated with green light. At pH 6.0 fluorescence increase and at pH 8.5 fluorescence decrease is observed showing pH dependent bidirectional proton transport. As a control, the same experiment was carried out using the D97N mutant which does not show any transport activity.

Our experiment confirms bidirectional proton transport by green PR as shown by Friedrich et al. [4]. The proton transport inverses in the physiological range around the pK_a of PR. The suggested experimental approach offers a qualitative complementation to black lipid membrane measurements. It seems surprising, that the fluorescence change at pH 6 is larger than at pH 8.5. Reasons could be differences in the net orientation and the nonlinear pH dependent quantum yield of HPTS. In addition, alkalinisation of the intracellular site of PR could restrict proton transfer [22].

2.2. Structure and oligomerisation studies: EM, AFM and solid-state NMR

Although PR has been well characterised by optical and IR spectroscopy, a 3D structure has not been reported yet but homology modelling based on the similarities to bacteriorhodopsin and sensory rhodopsin has been carried out and serves as a tool for the design

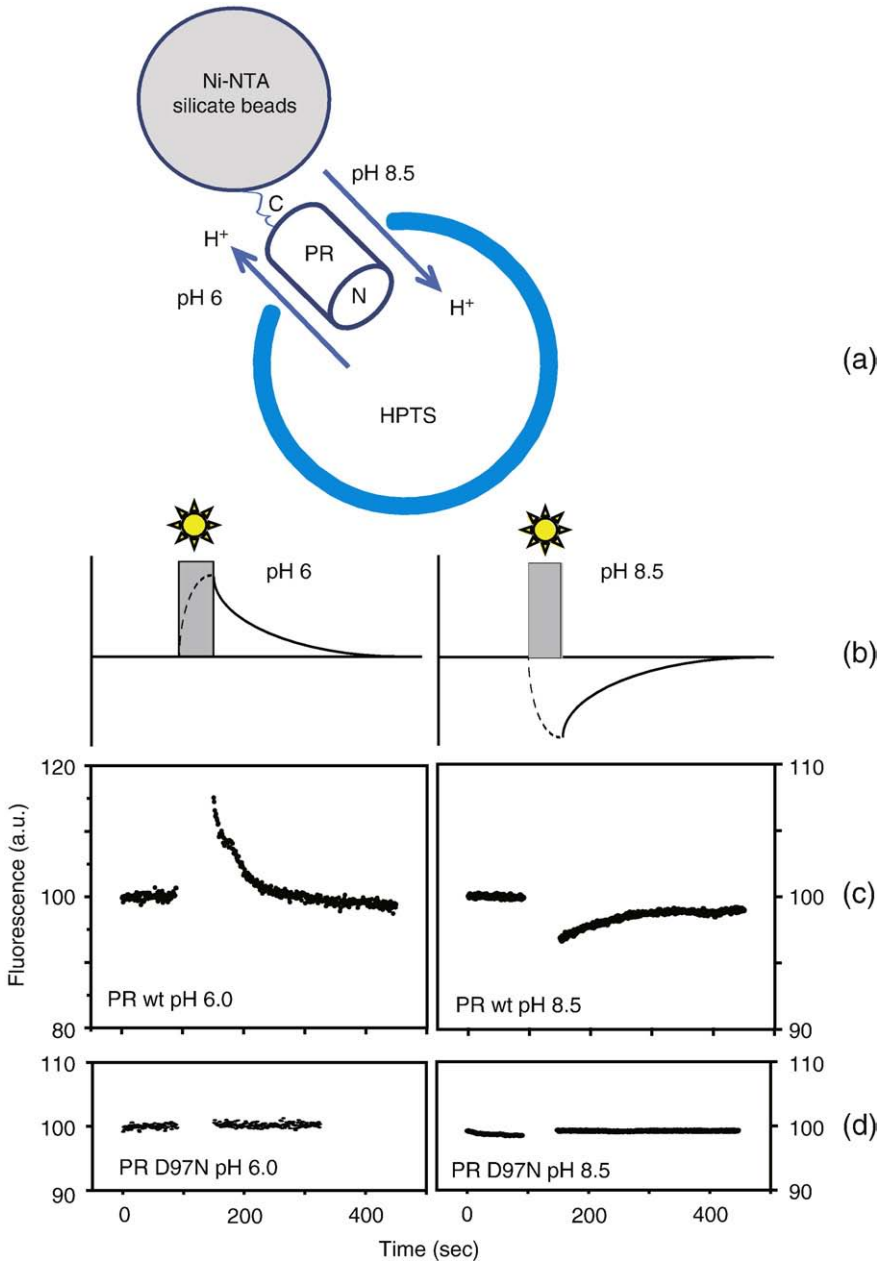

Fig. 2. Silicate beads covered with linked Ni–NTA groups were used to reconstitute His-tagged PR (C-terminal) in an oriented manner into proteoliposomes containing the pH dependent fluorescent dye HPTS (a). After removal of the beads the proteoliposomes were illuminated with green light (grey bar) to activate the photo cycle and proton pumping. Depending on the pH, protons were either transferred out of the vesicles (pH 6, fluorescent increase) or to the inside (pH 8.5, fluorescent decrease). Afterwards the return to the pH equilibrium is observed (b). Activity measurements of PR wt and D97N proteoliposomes at pH 6.0 and 8.5 reconstituted with Ni–NTA silicate beads (c). No fluorescent signal can be detected during the illumination period. PR wt shows bidirectional transport, the net transport direction depending on the pH (fluorescence increase, proton export for pH 6; fluorescent decrease, proton import for pH 8.5). The D97N mutant shows no activity over the whole pH range (constant fluorescence intensity) (d).

and interpretation of spectroscopic experiments and site-directed mutagenesis [4,5,23].

In collaboration with W. Kühlbrandt, Frankfurt, we have carried out an extensive 2D crystallization screen on PR [17]. The aim was a structure analysis based on cryo-EM as well as solid-state NMR. 2D crystallization is a attractive option to achieve high protein concentrations for solid-state NMR. Higher concentrations have been achieved for example by preparing 3D crystals of the membrane protein DGK [24] or by precipitating the transmembrane enzyme DsbB [25]. However, the best way to ensure a membrane environment at high protein concentration is 2D crystallisation, as demonstrated for the β-barrel outer-membrane porin OmpG [26].

Our crystallisation screen has shown that it is possible to crystallize PR under wide variety of a few hundred conditions. The poorly diffracting low quality 2D crystals were highly reproducible. The pH of the dialysis buffer and detergent for solubilisation of lipid and the protein played a crucial role. The interesting aspect of the 2D crystal of PR was the ability to crystallize under a wide range of different conditions and to produce similar quality of diffraction pattern. The most likely explanation could be that the protein has the tendency to associate or adhere by itself. Such a case is suggestive of strong protein–protein interaction. Diffraction data revealed a hexagonal lattice constant of 8.7 nm showing a symmetric ring like arrangement (Fig. 3a) indicating a higher oligomeric state. It has been reported that a large number of PR molecules exist per bacterial cell ($\sim 2.4 \times 10^4$) [27]. This fact together with our observation that 2D crystals form easily under many conditions could mean that PR might form protein patches in the native membrane.

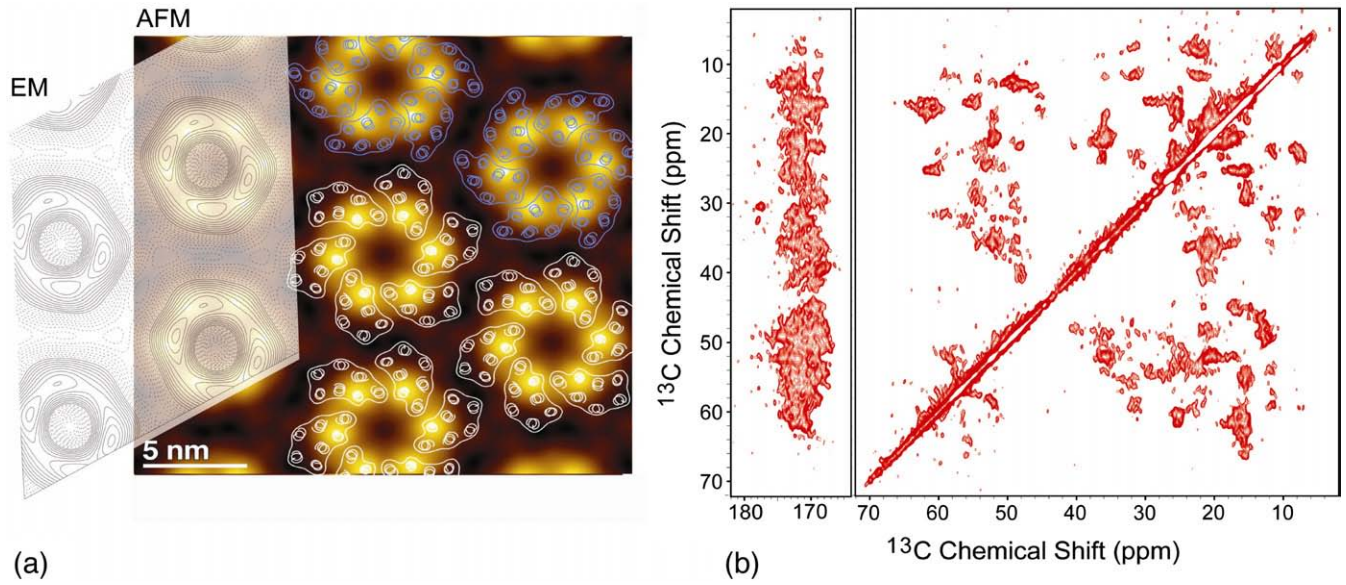

Fig. 3. PR has been found to form 2D crystals under many conditions. A low-resolution cryo-EM projection map in negative stain [17] revealed a ring-shaped assembly. It was shown by AFM image analysis of crystalline and non-crystalline sample preparations, that these rings are mainly formed by PR hexamers [16] (a). It can be hypothesized, that the protein could then be radially arranged. Densely packed or 2D crystalline samples of PR could be well suited for structural analysis by solid-state NMR (b). A 2D ^{13}C–^{13}C DARR (50 ms mixing time) spectrum of U–^{13}C, ^{15}N proteorhodopsin at 850 MHz and 14 kHz sample spinning shows that typical line-width of the isolated peaks in the spectrum is 0.5–0.7 ppm (see text).

The assumption of protein–protein contacts is also supported by CD spectroscopy on 2D crystals: a much higher protein stability in 2D crystals compared to detergent solubilised samples has been observed [28]. Under heat denaturing, 2D crystalline PR did show a sharp transition at ca. 70 °C while detergent solubilised PR gradually decayed with increasing temperature. In rapid-scan FTIR experiments, an M intermediate of the photocycle at basic pH could also be identified. We conclude that the Proteorhodopsin 2D crystals exhibit a fully functional photocycle and are therefore well suited for further studies on the proton transport mechanism of PR and for solid-state NMR experiments.

Reconstituted samples of PR were also analysed by AFM in cooperation with D.J. Müller, Dresden. Using single-molecule microscopy and force spectroscopy, it was observed that the ring-shaped PR structures observed by EM are actually mainly formed from hexamers [16]. A comparison is shown in Fig. 3a. The samples contain both crystalline and densely packed non-crystalline areas. By analyzing the non-crystalline areas, it has been shown that PR predominantly assembles into hexameric oligomers, but with a smaller fraction assembling into pentamers. This assembly is different from bacteriorhodopsin which is found to form trimers in a hexagonal array [29]. But force spectroscopy shows identical unfolding patterns with those of bacteriorhodopsin and halorhodopsin, which lets us conclude that PR folds similarly to archaeal rhodopsins.

2.2.1. Results and discussion

Besides biophysical-, hypothesis-driven structure-function studies, solid-state NMR holds also potential in 3D structure determination of insoluble macromolecules. A ^{13}C–^{13}C dipolar assisted rotational resonance (DARR) experiment [30] on a 2D crystalline U-^{13}C labelled PR sample is shown in Fig. 3b. Due to the dense sample packing, such a spectrum can be obtained within a reasonable amount of time. A mixing time of 50 ms was selected in order to pronounce through-space correlations between directly bonded nuclei. The typical line-width of isolated peaks in the spectrum is between 0.5 and 0.7 ppm which is a suitable starting point for further 2D and 3D solid-state NMR spectroscopy studies to probe structure and dynamics of PR.

Although PR seems to form 2D crystals under many conditions, it has not been possible to obtain well diffracting crystals. Reasons could be the inhomogeneous coexistence of small crystalline and larger non-crystalline areas, the coexistence of hexamers and pentamers or other reasons which cause sample inhomogeneity or instability. It has been suggested that the three Cys 107, 156 and 175 are involved in posttranslational modifications [31], which was not confirmed in the expression system used by us as they could be chemically modified for ^{19}F MAS NMR [32]. However, the first 18 N-terminal residues in the PR construct based on the cDNA of proteorhodopsin as found in the database (gene accession number AF279106, Q9F7P4) [4] is recognized as a signal peptide sequence by programmes such as SignalP (http://www.cbs.dtu.dk/services/SignalP/). This peptide would form an eighth transmembrane helix as predicted by TMHMM (http://www.cbs.dtu.dk/services/TMHMM/) (Fig. 4b) if it is not or not completely cleaved off in the *E. coli* expression system. This could have implications for data interpretation and sample preparation including crystallography.

We have probed whether this signal peptide is still attached to purified and reconstituted PR expressed in *E. coli* by creating a unique spin pair at position V10 and I11 (Fig. 1) through amino acid specific isotope labelling. By preparing a ^{13}C-Val/^{15}N-Ile PR sample, ^{13}C/^{15}N magnetisation transfer could only take place between V10 and I11 if a significant fraction of the sample still carries this signal peptide. Fig. 4c shows a conventional ^{13}C-CP MAS spectrum which arises from all 21 valine resonances in PR. A ^{15}N–^{13}C cross polarisation spectrum is shown in Fig. 4d. Here, only signal from V10 is observed, which proves, that a significant proportion of PR molecules still carry the signal peptide. Our observation agrees with the MALDI-TOF analysis in which the presence of two different species of PR molecules — with and without the extended N-terminus, was detected [4]. This sample inhomogeneity could explain the fact that low-resolution 2D crystals were obtained under a wide range of conditions but no high-resolution 2D crystals were formed.

2.3. New insight into the photo-active site: H75 and bound water

Solid-state NMR is an excellent tool to resolve molecular details of active sites in membrane proteins and significant amount of work has been done on bacteriorhodopsin [33]. We have reported the first solid-state NMR study to characterise the photoactive centre of PR [18]. The ^{13}C chemical shifts of 10,11-^{13}C retinal show unambiguously that

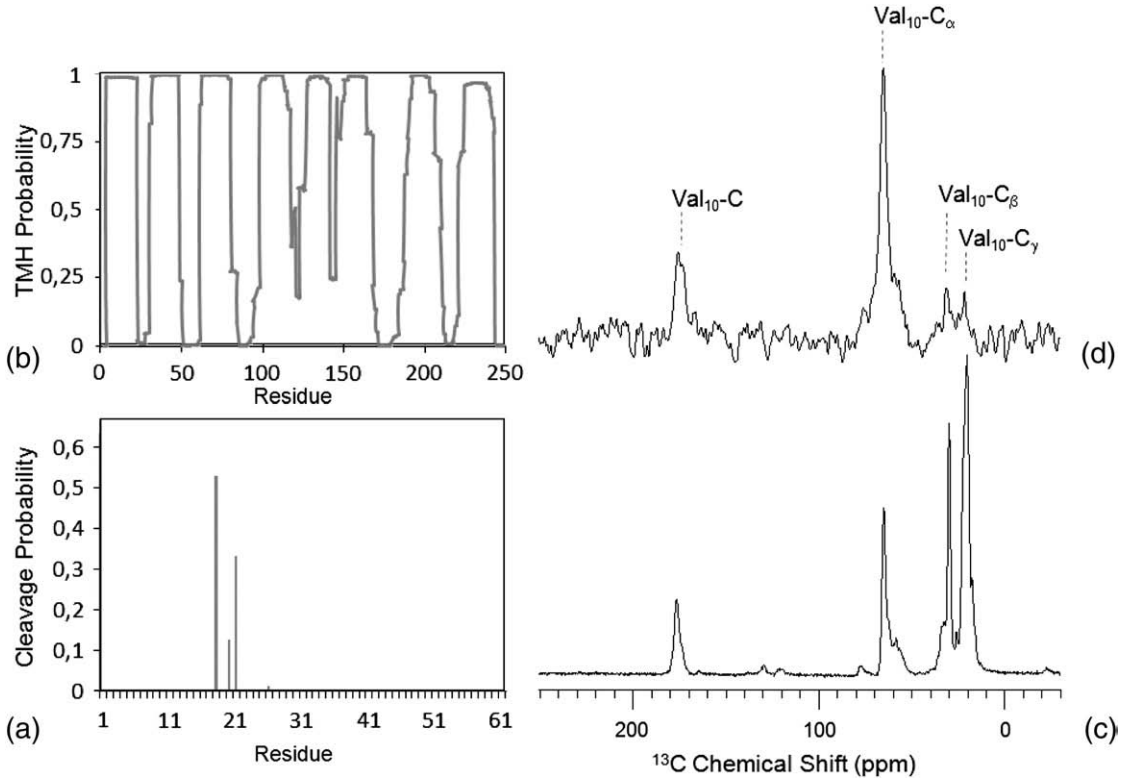

Fig. 4. The PR gene construct (Q9F7P4) used here contains an N-terminal sequence which is predicted by SignalP to be a signal peptide with a potential peptide cleavage site for Gram-negative bacteria between residues 17 and 18 (a). This signal peptide could form an additional transmembrane helix as predicted by TMHMM if it is not or only partially cleaved (b). In this signal peptide sequence, V10 and I11 form a unique pair. In a ^{13}C-Val/^{15}N-Ile-PR sample, a ^{13}C–^{15}N magnetization transfer between these residues would only be observable, if the signal peptide is not cleaved off. Overlapping signals from all 21 valine resonances are seen in a ^{13}C cross polarization experiments (c) while ^{13}C/^{15}N double cross polarization reveals signal from V10 only (d). This proves, that a significant proportion of PR molecules in the sample still carries the signal peptide which could have an effect onto sample homogeneity and crystal quality.

ground state PR only contains all-*trans* retinal. The ^{15}N chemical shift of the protonated Schiff base K231 provides an indication of a strong counterion interaction. The correlation the ^{15}N CS and the optical absorption maximum further indicates additional charges or constraints on the retinal conformation. The existence of a strong coupling network in the Schiff base vicinity is also supported by the high pH stability of the pSB chemical shift, which is weakened in the D97N mutant. Here, we show new NMR data showing bound water in the photoactive site and we report results towards the elucidation of the role of highly conserved H75.

3. Results and discussion

3.1. The role of H75

This histidine at position 75 is close to the middle of helix B, in close proximity to the photoactive centre and could be of functional importance [5,34]. The pK_a of histidine is in the physiological range. Therefore, its imidazole group is often involved in proton transfer reactions and could be responsible for stabilizing the high pK_a of the proton acceptor D97 in PR. In BR, a Met is found at this position (Fig. 1). Here, we report the effect of single site mutations H75M, N and W onto the optical absorption and the ^{15}N chemical shift of the pSB.

Our data show that mutation of H75 does not influence the ^{15}N CS of the pSB (181.5 ppm) although in the case of H75W, a significant signal reduction is observed which could arise from a partial deprotonation of the Schiff base at alkaline pH (Fig. 5a). UV–VIS absorption spectra at different pH were acquired for all three mutants in reconstituted form in order to determine the pK_a of the chromophore. The absorption maximum was obtained after correcting the absorption spectra for light scattering. The pK_a values were determined to be 6.3 (H75M), 5.3 (H75W) and 4.4 (H75N) as shown in Fig. 5b, which deviates significantly from the wild type at 7.5 [4]. Since the pK_a of the chromophore is correlated with the pK_a of the proton acceptor D97, it can be concluded, that H75 interacts with D97. The proximity of H75 to D97 in a BR-based model of PR has been already suggested by Rangarajan et al. [5,34]. The absorption maximum for H75M, W and N at pH 8.5 in DOPC liposomes after correction of light scattering were 517, 518 and 528 nm. The fact that the λ_{max} is different for different mutations has also been reported by Bergo et al. [34] for the case for H75A and H75E and can be explained by a perturbed structure of the active site.

In order to interpret our findings, we tried to correlate the Schiff base ^{15}N chemical shifts with λ_{max}. Protonated Schiff bases of retinal derivatives with all-*trans* polyene chains with different halide counterions show a proportional relationship of the maximum wavelength and the ^{15}N chemical shift of the pSB [35]. Proteorhodopsin shows a much stronger deviation from this relationship than all-*trans* BR (BR$_{568}$) for the wt as well as the D97N mutant and the H75 mutants (Fig. 5c), which shows that additional factors must contribute to this red shift, such as twisting around double bonds within the retinal or negative charges close to the chromophore [35,36].

3.2. Detection of bound water in the photoactive site of PR

Previously, we were able to show by ^{15}N-CP-MAS NMR, that the pK_a of the Schiff base K231 is relatively high (~pH 12) [18]. One possible explanation for this observation could be a high dielectric constant in the vicinity of the Schiff base as it would arise from water molecules which form part of the SB counterion complex. Bound water molecules play generally an important role in the distribution and transfer of charges in proteins. They are especially important for

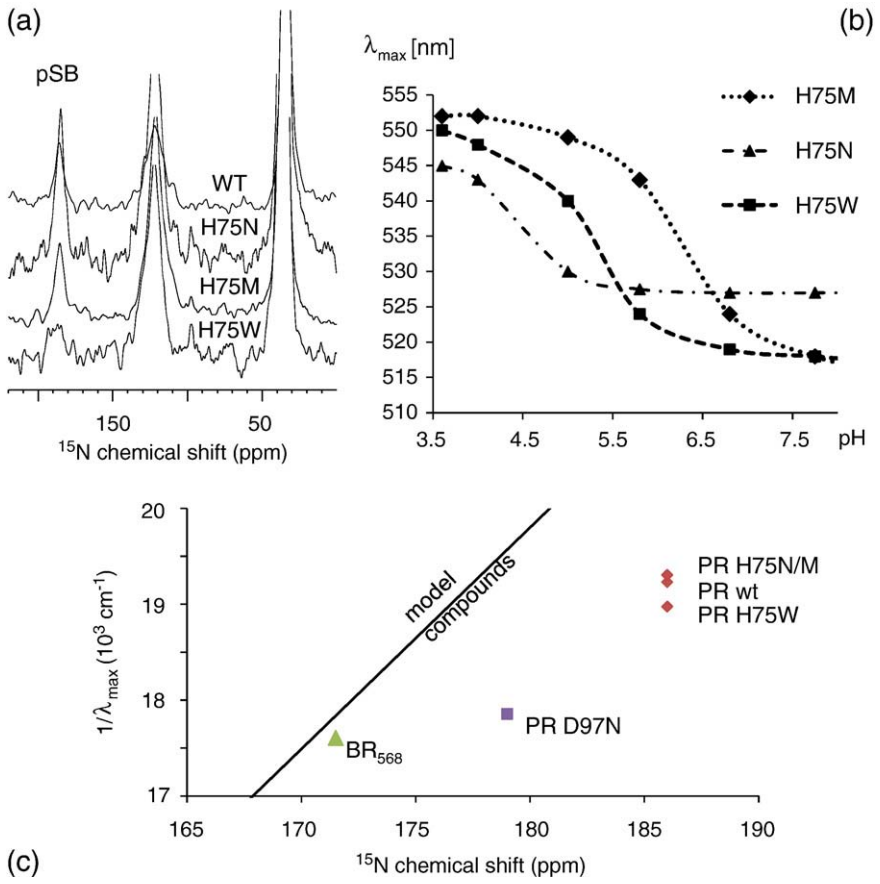

Fig. 5. The effect of H75 single site mutations onto the chromophore properties has been investigated. Both ^{15}N CS and λ_{max} were measured in proteoliposomes (DOPC). The ^{15}N chemical shift of the pSB in wt ^{15}N-ζ-Lys PR compared to H75N, M, W is not affected at pH8.5, but a strongly reduced signal intensity for the pSB is observed for H75W (a). The pSB is observed at 181.5 ppm, backbone resonances are seen around 118.5 ppm and lysine side chains at 32.5 ppm. Slightly more pronounced effects are observed for λ_{max} and the pK_a of the chromophore (b). For H75M, W and N, a λ_{max} at alkaline pH is found at 517, 518 and 528 nm and pK_a values of 6.3, 5.3 and 4.4 were determined. pSB ^{15}N chemical shift data and absorption maxima are compared for PR wt, D97N, H75N, M and W with BR_{568} and retinal derivatives with all-*trans* polyene chains with different halide counterions. Proteorhodopsin shows a much stronger deviation from this linear relationship than all-trans BR (BR_{568}) for the wt as well as the D97N mutant. However the H75 mutants are similar to wt PR indicating that there is no direct interaction between H75 and the pSB. The figure was adopted from Hue et al. [18,35] and Pfleger et al. [18,35].

the function of proton pumps [33]. Based on FTIR studies, the existence of a bound water cluster in the alkaline form of PR [37] has been suggested. Here, we show that indeed bound water exist in close proximity to the pSB.

We have carried out ^{15}N–^{1}H HETCOR experiments with homonuclear frequency-switched Lee–Goldburg [38] decoupling in the ^{1}H dimension on ^{15}N-ζ-Lys PR at pH 8.5. Through space correlations between the pSB and neighbouring protons, e.g. arising from H_2O, should be well observable, as its ^{15}N chemical shift at 181.5 ppm is well separated from the backbone lysine side chain resonances (Fig. 5a). A correlation between ^{15}N and ^{1}H in the pSB is shown in Fig. 6a. The Schiff base proton resonates between 9 and 10 ppm. This spectrum was acquired using a very short cross polarization contact time of 200 μs by which mainly magnetization from very close protons with strong ^{1}H–^{15}N dipolar couplings is transferred to the ^{15}N nuclei. More distant protons can be probed by longer CP contact times. Extending the contact time to 2 ms, correlations between the pSB nitrogen and protons at 3.2 and 5.2 ppm are observed (Fig. 6b). The latter chemical shift is in a range expected for water [39,40], while the other peak arises most likely from the H_ε in lysine. In order to verify our findings, a deuterium exchange experiment has been carried out. The resonance at 5.2 ppm disappears and the pSB ^{15}N resonance is shifted to 178.5 ppm (Fig. 6c). This supports our finding that the 5.2 ppm resonance arises from water bound close to the pSB and not from H_{14} in the retinal for which a similar chemical shift in BR has been observed [41] but which would not be exchangeable.

Our data suggest that water is located close to the SB which could be essential for proton transfer if this water molecule is involved e.g. in a hydrogen bond with the pSB. A small deuterium isotope effect on the pSB ^{15}N chemical shift of +3 ppm ($^{15}N(H)$–$^{15}N(D)$) has been observed and can be compared with data from model compounds such as pyridine which have delocalized π electrons and a protonable nitrogen [42]. In the case of pyridine interacting with different kind of deuterated and protonated acids the ^{15}N isotope shift was negative for weak acids (meaning that the proton of the hydrogen bonded complex is closer to the acid) and positive for strong acids (meaning that the proton of the hydrogen bonded complex is closer to the pyridine). In the case of strong acids the isotope effect ranges up to 8 ppm. Considering pyridine to be a model compound for the SB due to the delocalized pi electrons and the protonable nitrogen our positive isotope effect of ~3 ppm indicates that the SB proton is closer to the SB. The relatively small isotope effect of ~3 ppm compared to 8 ppm however could arise from the formation of a hydrogen bond to an electron donor like water oxygen which would also explain the larger ^{15}N chemical shift of the pSB in PR compared to BR [18].

3.3. Conclusion and outlook

Proteorhodopsins are fascinating proteins. Understanding their functional role, structure and mechanism has potentially a high impact for the understanding of bioenergetic processes within marine ecosystems. We were able to provide additional evidence for the proton transport characteristics of PR *in vitro* and a first insight into

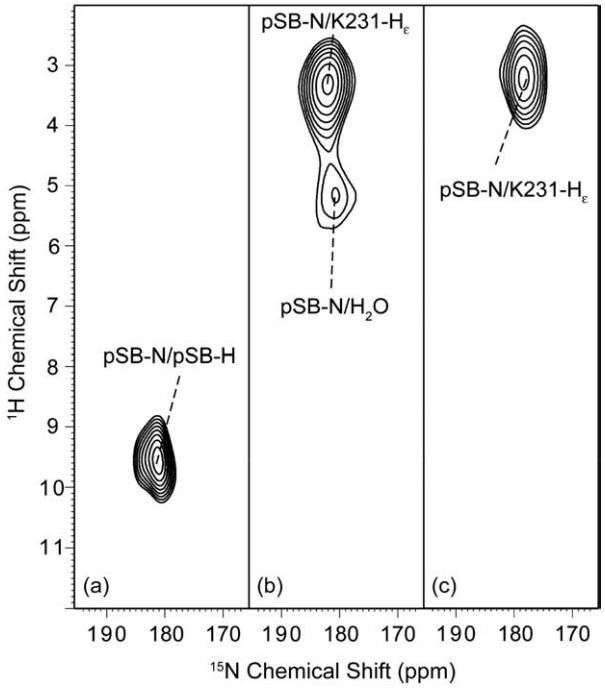

Fig. 6. ^{15}N–^{1}H correlation of ^{15}N ζ-lysine labeled PR in H_2O (a,b) and D_2O (c) at the ^{15}N CS of the pSB. In (a) the CP contact time was set to only 200 μs in order to observe only the directly bound proton to the pSB. In (b) (H_2O) and (c) (D_2O) the contact time was 1500 μs to observe signals of protons at a distance range of 2–4 Å. In both H_2O and D_2O the $C_ε$–H resonance of K231 can be observed whereas the proton CS at ~5 ppm disappears in D_2O suggesting the presence of water close to the pSB. The ^{15}N CS of the pSB was shifted by 3 ppm (178.5 ppm) due to the isotope effect after (H/D) exchange.

the packing and assembly of PR within lipid bilayers has been obtained. Based on these data we postulate a dense packing of PR also *in situ*. Significant progress still has to be made in order to resolve the 3D structure of PR and NMR spectroscopic approaches will offer an alternative in addition to crystallography. Especially solid-state NMR is well suited for hypothesis-driven biophysical studies. We were able to provide direct evidence for bound water within the retinal binding pocket close to the pSB, which could explain its high pK_a. The first glance at the role of H75 has been obtained indicating a direct interaction with D97 rather than the Schiff base. A more detailed study on the interaction of H75 with neighbouring residues is in progress and will be reported elsewhere.

4. Materials and methods

4.1. Used plasmids and strains

PR (wt, D97N) was cloned in the pET27b(+) [4] vector which was transformed in the *E. coli* strain C41 (DE3). The same vector was used for H75N, M and W mutants, but with transformation into *E. coli* strain C43 (DE3). The PR wt and D97N pET27b(+) vector has been kindly provided E. Bamberg, MPI of Biophysics, Frankfurt.

4.2. Proteorhodopsin H75X mutants

Single point mutations of PR wt into H75N, H75M and H75W have been created by PCR on the wild type plasmid and with the help of mismatch primers (5′GGTATTGCTTTCTGG-ATG-TACATGTACATGA-GAGGGG3′ and complementary reverse for H75M, others similar). After multiplication of the complete, but mutated plasmid the original methylated plasmid became digested by DpnI for 1 h at 37 °C. The correct mutations have been verified by sequence analysis of the complete PR gene.

4.3. Expression and purification of PR was essentially carried out as described previously [17,18]

Escherichia coli cells were grown at 37 °C in defined medium with unlabelled amino acids with 50 μg/mL kanamycine to an OD_{578} of ~0.8. After spinning down, cells were resuspended in fresh medium containing labelled ^{15}N ζ-lysine for probing the SBs CS and for the HETCOR experiment (Fig. 6) and with $U^{13}C$-valine + ^{15}N-isoleucine for probing for the presence of the N-terminus (Fig. 4), respectively. After 15 min of incubation, 1 mM IPTG and 0.7 mM of all-*trans* retinal dissolved in ethanol were added. For the DARR measurements (Fig. 3), PR was grown and induced in minimal medium with ^{13}C glucose and ^{15}N NH_4SO_4. Overexpression was achieved by a further incubation at 37 °C for 3–4 h and was visually observed by a pink colour change of the cells. Cells were harvested by centrifugation and broken using a Constant System cell disrupter at 1.5–2 kbar. The recovered membrane pellet was solubilised with 1.5% DDM overnight. Detergent solubilised PR (supernatant) was obtained by ultra-centrifugation and was incubated with Ni–NTA beads for approximately 1 h. After thorough washing, the protein was finally eluted in 0.2% Triton X-100. Purity of preparation was checked on SDS PAGE.

4.4. Oriented reconstitution of PR with Ni–NTA silicate particles (Fig. 2)

0.1% DDM solubilized His-tagged PR was incubated with Ni–NTA coated silicate particles (Kisker Biotech) with a diameter of 0.2 μm containing 50 nmol/mL NTA groups for 30 min in 300 mM NaCl, 50 mM MES, pH 7.5 under slight shaking. Unbound protein was removed by centrifugation for 5 min in a table centrifuge at 3000 *g* in the supernatant (density of silicate particles is 2 mg/mL). Liposomes were formed by an extruder with 10 mg/mL POPC/POPG (5:1 mol/mol) in 150 mM KCl, 0.5 mM glycylglycine and 1 mM HPTS at pH 8.5. The lipid solution was filtered 5× with a 500 nm and 200 nm filter each (Nucleopore Track-Etch Membrane, Whatmann). The liposomes were solubilized for reconstitution with 6.6 mg/mL DDM (in total) for 60 min. The silicate bound PR molecules were added to the solubilized liposome solution (PR/lipids 1:500 mol/mol) and slightly shaked for 15 min. 200 mg/mL biobeads were added for fast desolubilization during 30 min. Then the biobeads were removed and 500 mM imidazole (pH 8.5) was added to release the Ni–NTA silicate particles, which were removed by centrifugation (5 min, 3000 *g*). Proteoliposomes were sedimented in a Beckmann ultracentrifuge at 220,000 *g* for 30 min, dissolved in and dialysed against 150 mM KCl, 0.5 mM glycylglycine, pH 8.5 to remove residual HPTS outside of the vesicles.

4.5. Reconstitution for solid-state NMR spectroscopy

2D Crystals were produced as described previously (at pH8.5 in DOPC, [17,18]).

4.6. Optical spectroscopy

UV/VIS spectra (Fig. 5) of reconstituted (DOPC) PR were acquired on a Jasco V-550 spectrophotometer. Spectra of the mutants H75M, H75N and H75W were measured in three different buffers: pH 3.5 (50 mM NaAc), pH4 (50 mM NaAc), pH5 (50 mM NaAc), pH 6 (50 mM MES), pH7 (50 mM HEPES), pH 8 (50 mM Tris) and pH9 (50 mM Tris). Light scattering was subtracted by an exponential fit. Fluorescence transport measurements (Fig. 2) were performed on a Jasco Spectrofluorimeter FP-6500 at 25 °C. The proteoliposomes were illuminated with a cold light lamp KL 1500 LCD from Zeiss with a green filter from outside in a solution of 150 mM KCl and 0.5 mM glycylglycine, starting from pH 8.5. HPTS fluorescence was excited at 460 nm with a slit width of 3 nm and recorded at 514 nm with a sensitivity of 300–700 V. After adaption of the pH the 514 nm signal was followed until equilibration.

4.7. Solid-state NMR

The 2D ^{13}C–^{13}C DARR spectrum (Fig. 3b) was acquired on a wide-bore Bruker Avance III 850 MHz solid-state NMR spectrometer equipped with a 4 mm DVT probehead. A mixing time of 50 ms, 512 increments in the t1 dimension with 64 scans each were used. The spinning speed was set to 14 kHz. The actual sample temperature during the experiment was 278 K. Chemical shift referencing was carried out with respect to TMS through adamantine (resonances at 38.56 and 29.5 ppm).

^{15}N CP MAS-NMR CP experiments (Fig. 5a) were carried out on a Bruker Avance 600 equipped with a 4 mm MAS DVT probehead. Cross polarization experiments were performed at 60.88 MHz for ^{15}N. An 80–100% ramped proton pulse of 1.5 ms was used during the Hartmann–Hahn match. Proton decoupling of 90 kHz was applied during a 50 ms acquisition time. The recycle delay time was 2 s. The measurements were carried out at a sample spinning of 10 kHz at 225 K. The ^{15}N chemical shifts were referenced indirectly with respect to the virtual zero point of liquid ammonia through the absolute ^{13}C frequency at 0 ppm and the standardized gyromagnetic ratios of ^{13}C and ^{15}N. Adamantane was used as a secondary ^{13}C chemical shift standard with 38.56 ppm for the $^{13}CH2$ resonance. Please note, that this causes a chemical shift difference of −4.5 ppm for ^{15}N data reported by us previously [17,18] using another chemical shift calibration.

^{13}C detected ^{1}H–^{15}N–^{13}C-DCP (double cross polarisation) experiments were performed at a Bruker Avance II 400 equipped with a 4 mm MAS DVT probehead. Magnetization first was transferred from ^{1}H to ^{15}N by a usual CP step. An 80–100% ramped proton pulse of 0.6 ms was used during the ^{1}H–^{15}N Hartmann–Hahn match. For the second ^{15}N–^{13}C CP step a contact time of 4.5 ms was used while the protons were decoupled at 90 kHz. During the acquisition a 85 kHz two pulse phase modulation proton decoupling was used. Spectra were referenced externally to the ^{15}N resonance of solid ^{15}N ammonium sulphate at 27 ppm and to the ^{13}C signal of TMS at 0 ppm.

The ^{15}N–^{1}H HETCOR experiments with CP magnetisation transfer (Fig. 6) [38] were acquired at 225 K using 10 kHz sample spinning using an Bruker Avance 400 spectrometer and a 4 mm DVT probehead. During the evolution period frequency-switched Lee–Goldburg decoupling was applied at an effective proton decoupling field of 80 kHz. A refocusing ^{15}N pulse was applied during evolution [40]. During the acquisition period two pulse phase modulation proton decoupling was used at 70 kHz. 13 k scans were recorded with 32 increments in the indirect dimension. For D_2O exchange, samples were resuspended to deuterated buffer for 1 h under white light illumination, pelleted and collected for NMR measurements. The ^{1}H chemical shift scaling factor and calibration was determined experimentally by comparing ^{13}C–^{1}H HETCOR spectra of DMPC with and without homonuclear proton decoupling during t1.

Acknowledgement

This work has been financially supported by SFB 472 (“Molecular Bioenergetics”). We deeply acknowledge excellent cooperation and many helpful discussions throughout this funding period with our partners Ernst Bamberg, Werner Kühlbrandt, Janet Vonck, Winfried Haase (MPI Biophysics, Frankfurt), Thomas Friedrich (TU Berlin), Martin Engelhardt (MPI Physiology, Dortmund), Josef Wachtveitl, Werner Mäntele (Goethe University, Frankfurt) and Daniel Müller (TU Dresden). We appreciate help with site-directed mutagenesis by Sarah-Anna Fiedler and maintenance of the NMR spectrometers by Jakob J. Lopez and Christoph Kaiser.

References

[1] O. Beja, L. Aravind, E.V. Koonin, M.T. Suzuki, A. Hadd, L.P. Nguyen, S.B. Jovanovich, C.M. Gates, R.A. Feldman, J.L. Spudich, E.N. Spudich, E.F. DeLong, Bacterial rhodopsin: evidence for a new type of phototrophy in the sea, Science 289 (2000) 1902–1906.
[2] G. Sabehi, A. Loy, K.H. Jung, R. Partha, J.L. Spudich, T. Isaacson, J. Hirschberg, M. Wagner, O. Beja, New insights into metabolic properties of marine bacteria encoding proteorhodopsins, PLoS Biol. 3 (2005) e273.
[3] W.W. Wang, O.A. Sineshchekov, E.N. Spudich, J.L. Spudich, Spectroscopic and photochemical characterization of a deep ocean proteorhodopsin, J. Biol. Chem. 278 (2003) 33985–33991.
[4] T. Friedrich, S. Geibel, R. Kalmbach, I. Chizhov, K. Ataka, J. Heberle, M. Engelhard, E. Bamberg, Proteorhodopsin is a light-driven proton pump with variable vectoriality, J. Mol. Biol. 321 (2002) 821–838.
[5] R. Rangarajan, J.F. Galan, G. Whited, R.R. Birge, Mechanism of spectral tuning in green-absorbing proteorhodopsin, Biochemistry 46 (2007) 12679–12686.
[6] J.M. Walter, D. Greenfield, C. Bustamante, J. Liphardt, Light-powering *Escherichia coli* with proteorhodopsin, Proc. Natl. Acad. Sci. U. S. A. 104 (2007) 2408–2412.
[7] J.A. Fuhrman, M.S. Schwalbach, U. Stingl, Proteorhodopsins: an array of physiological roles? Nat. Rev. Microbiol. 6 (2008) 488–494.
[8] A.K. Dioumaev, L.S. Brown, J. Shih, E.N. Spudich, J.L. Spudich, J.K. Lanyi, Proton transfers in the photochemical reaction cycle of proteorhodopsin, Biochemistry 41 (2002) 5348–5358.
[9] V. Bergo, J.J. Amsden, E.N. Spudich, J.L. Spudich, K.J. Rothschild, Structural changes in the photoactive site of proteorhodopsin during the primary photoreaction, Biochemistry 43 (2004) 9075–9083.
[10] R. Huber, T. Kohler, M.O. Lenz, E. Bamberg, R. Kalmbach, M. Engelhard, J. Wachtveitl, pH-dependent photoisomerization of retinal in proteorhodopsin, Biochemistry 44 (2005) 1800–1806.
[11] E.S. Imasheva, S.P. Balashov, J.M. Wang, A.K. Dioumaev, J.K. Lanyi, Selectivity of retinal photoisomerization in proteorhodopsin is controlled by aspartic acid 227, Biochemistry 43 (2004) 1648–1655.
[12] M.O. Lenz, R. Huber, B. Schmidt, P. Gilch, R. Kalmbach, M. Engelhard, J. Wachtveitl, First steps of retinal photoisomerization in proteorhodopsin, Biophys. J. 91 (2006) 255–262.
[13] M.O. Lenz, A.C. Woerner, C. Glaubitz, J. Wachtveitl, Photoisomerization in proteorhodopsin mutant D97N, Photochem. Photobiol. 83 (2007) 226–231.
[14] K. Neumann, M.K. Verhoefen, I. Weber, C. Glaubitz, J. Wachtveitl, Initial reaction dynamics of proteorhodopsin observed by femtosecond infrared and visible spectroscopy, Biophys. J. 94 (2008) 4796–4807.
[15] G. Varo, L.S. Brown, M. Lakatos, J.K. Lanyi, Characterization of the photochemical reaction cycle of proteorhodopsin, Biophys. J. 84 (2003) 1202–1207.
[16] A.L. Klyszejko, S. Shastri, S.A. Mari, H. Grubmuller, D.J. Muller, C. Glaubitz, Folding and assembly of proteorhodopsin, J. Mol. Biol. 376 (2008) 35–41.
[17] S. Shastri, J. Vonck, N. Pfleger, W. Haase, W. Kuehlbrandt, C. Glaubitz, Proteorhodopsin: characterisation of 2D crystals by electron microscopy and solid state NMR, Biochim. Biophys. Acta 1768 (2007) 3012–3019.
[18] N. Pfleger, M. Lorch, A.C. Woerner, S. Shastri, C. Glaubitz, Characterisation of Schiff base and chromophore in green proteorhodopsin by solid-state NMR, J. Biomol. NMR 40 (2008) 15–21.
[19] A.K. Dioumaev, J.M. Wang, Z. Balint, G. Varo, J.K. Lanyi, Proton transport by proteorhodopsin requires that the retinal Schiff base counterion Asp-97 be anionic, Biochemistry 42 (2003) 6582–6587.
[20] M. Lakatos, J.K. Lanyi, J. Szakacs, G. Varo, The photochemical reaction cycle of proteorhodopsin at low pH, Biophys. J. 84 (2003) 3252–3256.
[21] N.R. Clement, J.M. Gould, Pyranine (8-Hydroxy-1,3,6-Pyrenetrisulfonate) as a probe of internal aqueous hydrogen-ion concentration in phospholipid-vesicles, Biochemistry 20 (1981) 1534–1538.
[22] R. Hagedorn, D. Gradmann, P. Hegemann, Dynamics of voltage profile in enzymatic ion transporters, demonstrated in electrokinetics of proton pumping rhodopsin, Biophys. J. 95 (2008) 5005–5013.
[23] J.R. Hillebrecht, J. Galan, R. Rangarajan, L. Ramos, K. McCleary, D.E. Ward, J.A. Stuart, R.R. Birge, Structure, function, and wavelength selection in blue-absorbing proteorhodopsin, Biochemistry 45 (2006) 1579–1590.
[24] M. Lorch, S. Fahem, C. Kaiser, I. Weber, A.J. Mason, J.U. Bowie, C. Glaubitz, How to prepare membrane proteins for solid-state NMR: a case study on the alpha-helical integral membrane protein diacylglycerol kinase from *E. coli*, Chembiochem 6 (2005) 1693–1700.
[25] Y. Li, D.A. Berthold, H.L. Frericks, R.B. Gennis, C.M. Rienstra, Partial (13)C and (15)N chemical-shift assignments of the disulfide-bond-forming enzyme DsbB by 3D magic-angle spinning NMR spectroscopy, Chembiochem 8 (2007) 434–442.
[26] M. Hiller, L. Krabben, K.R. Vinothkumar, F. Castellani, B.J. van Rossum, W. Kuhlbrandt, H. Oschkinat, Solid-state magic-angle spinning NMR of outer-membrane protein G from *Escherichia coli*, Chembiochem 6 (2005) 1679–1684.
[27] O. Beja, E.N. Spudich, J.L. Spudich, M. Leclerc, E.F. DeLong, Proteorhodopsin phototrophy in the ocean, Nature 411 (2001) 786–789.
[28] G. Schäfer, S. Shastri, M.K. Verhoefen, V. Vogel, C. Glaubitz, J. Wachtveitl, W. Mäntele, Characterizing the structure and photocycle of PR 2D crystals with CD- and FTIR spectroscopy, Photochem. Photobiol. Science 85 (2009) 529–534.
[29] N. Grigorieff, T.A. Ceska, K.H. Downing, J.M. Baldwin, R. Henderson, Electron-crystallographic refinement of the structure of bacteriorhodopsin, J. Mol. Biol. 259 (1996) 393–421.
[30] K. Takegoshi, S. Nakamura, T. Terao, C-13-H-1 dipolar-assisted rotational resonance in magic-angle spinning NMR, Chem. Phys. Lett. 344 (2001) 631–637.
[31] R.A. Krebs, U. Alexiev, R. Partha, A.M. DeVita, M.S. Braiman, Detection of fast light-activated H+ release and M intermediate formation from proteorhodopsin, BMC. Physiol. 2 (2002) 5.
[32] U.A. Hellmich, N. Pfleger, C. Glaubitz, 19F-MAS NMR on proteorhodopsin: enhanced protocol for site-specific labeling for general application to membrane proteins, Photochem. Photobiol. Science 85 (2009) 535–539.
[33] J. Herzfeld, J.C. Lansing, Magnetic resonance studies of the bacteriorhodopsin pump cycle, Annu. Rev. Biophys. Biomol. Struct. 31 (2002) 73–95.

[34] V.B. Bergo, O.A. Sineshchekov, J.M. Kralj, R. Partha, E.N. Spudich, K.J. Rothschild, J.L. Spudich, His75 in proteorhodopsin, a novel component in light-driven proton translocation by primary pumps, J. Biol. Chem. (2008).
[35] J. Hu, R.G. Griffin, J. Herzfeld, Synergy in the spectral tuning of retinal pigments: complete accounting of the opsin shift in bacteriorhodopsin, Proc. Natl. Acad. Sci. U. S. A. 91 (1994) 8880–8884.
[36] J.G. Hu, B.Q. Sun, A.T. Petkova, R.G. Griffin, J. Herzfeld, The predischarge chromophore in bacteriorhodopsin: a 15N solid-state NMR study of the L photointermediate, Biochemistry 36 (1997) 9316–9322.
[37] D. Ikeda, Y. Furutani, H. Kandori, FTIR study of the retinal Schiff base and internal water molecules of proteorhodopsin, Biochemistry 46 (2007) 5365–5373.
[38] B.J. vanRossum, H. Forster, H.J.M. deGroot, High-field and high-speed CP-MAS C-13 NMR heteronuclear dipolar-correlation spectroscopy of solids with frequency-switched Lee–Goldburg homonuclear decoupling, J. Magn. Reson. 124 (1997) 516–519.
[39] G.Y. Cho, Y.T. Wu, J.L. Ackerman, Detection of hydroxyl ions in bone mineral by solid-state NMR spectroscopy, Science 300 (2003) 1123–1127.
[40] A. Lesage, L. Emsley, F. Penin, A. Bockmann, Investigation of dipolar-mediated water-protein interactions in microcrystalline Crh by solid-state NMR spectroscopy, J. Am. Chem. Soc. 128 (2006) 8246–8255.
[41] H. Patzelt, B. Simon, A. terLaak, B. Kessler, R. Kuhne, P. Schmieder, D. Oesterhelt, H. Oschkinat, The structures of the active center in dark-adapted bacteriorhodopsin by solution-state NMR spectroscopy, Proc. Natl. Acad. Sci. U. S. A. 99 (2002) 9765–9770.
[42] S.N. Smirnov, N.S. Golubev, G.S. Denisov, H. Benedict, P. SchahMohammedi, H.H. Limbach, Hydrogen deuterium isotope effects on the NMR chemical shifts and geometries of intermolecular low-barrier hydrogen-bonded complexes, J. Am. Chem. Soc. 118 (1996) 4094–4101.